

The Inner Source for Pickup Ions

N. A. Schwadron^a, G. Gloeckler^{a,b}, L. A. Fisk^a, J. Geiss^c, and T. H. Zurbuchen^a

^a*Department of Atmospheric, Oceanic and Space Science, University of Michigan, Ann Arbor, USA, 48109*

^b*Department of Physics and IPST, University of Maryland, College Park, USA, 20742*

^c*International Space Science Institute, Bern, Switzerland, CH-3012*

Abstract. Pickup ions are observed by the Solar Wind Ion Composition Spectrometer on Ulysses which appear to have been picked up close to the Sun. A transport theory for the propagation of these ions is used to constrain the spatial profiles of the ion sources. The composition is like that of the solar wind which suggests that the inner source pickup ions result from solar wind particles that are embedded in dust grains and then released. Through comparison between modeled and observed distributions, it is possible to constrain the radial and latitudinal profiles of the inner source. Inner source protons are also observed and may constitute an energetically important population in the solar wind.

INTRODUCTION

Neutral particles in the heliosphere may become ionized due to photoionization, electron impact ionization, or charge exchange. Subsequently such ions are readily picked up by the solar wind as they gyrate about the frozen-in magnetic field lines. Pickup ions can be produced from many sources: interstellar neutrals; comets; planets; and interstellar or interplanetary grains.

Recently pickup ions were identified which had been picked up close to the Sun, at less than 0.5 AU (2, 4). The ion species C^+ , O^+ , and N^+ were identified.

The composition of the inner source ions is like that of the solar wind, with H^+ , C^+ , N^+ , O^+ , Ne^+ , Mg^+ and Si^+ all having been identified as components of the inner source (see, (3) for a full discussion of the inner source abundances relative to that of the solar wind). Note in particular the presence of Ne^+ . Small dust grains in the heliosphere are not expected to contain volatile elements such as Ne, and may be depleted in H unless these particles are bound in molecular form. The presence of Ne and H in the inner source suggests strongly, and perhaps conclusively, that these particles originate as solar wind ions which are embedded and subsequently released from dust grains, eventually then becoming pickup ions. The physics involved in the embedding and release of solar wind ions is discussed in (7).

The purpose of this paper is to discuss the implications of inner C^+ and O^+ distribution functions for the radial and latitudinal profiles of the inner source, and to establish the presence and potential energetic importance of inner source H^+ . These topics are examined in detail in (11).

OBSERVATIONS

The pickup ion data presented here were obtained with the Solar Wind Ion Composition Spectrometer (SWICS) on the Ulysses satellite (5). The observed distribution functions of hydrogen, carbon, and oxygen are shown in Figure 1 for all of 1994. The observed distribution function, $\tilde{f}(v')$ can be related to the distribution function in the solar wind frame, $f(\mathbf{v})$ through an angular integration over the instrument acceptance angles. Here v' is the speed in the spacecraft reference frame and \mathbf{v} is the ion velocity in the solar wind reference frame.

During the observation period used in Figure 1, all of 1994, Ulysses moved between 48°S latitude to 80° and then back to 45°S. Ulysses also traveled from 3.8 AU to 1.6 AU. The solar wind speed was extremely steady with $u \sim 780$ km/s.

The second set of observations are shown in Figure 2 representing a period from day 30 to day 90 of 1995 while Ulysses moved rapidly between 25°S latitude to 20°N latitude climbing $\sim 1^\circ$ in latitude each day, as it remained near 1.4 AU. This was a unique opportunity to observe the inner source ions since Ulysses was closer to the Sun than at other points in its orbit. Ulysses experienced at least half a dozen fast and slow streams during this period as the solar wind varied between 300 km/s and 750 km/s.

A MODEL

Although the inner source for pickup ions is a topic explored only recently, the study of interstellar pickup ions provides constraints and clues for the transport of inner

Table 1. Parameters used for modeling the inner source. In the fourth and fifth columns we list $dm/dt(r_1)$ in units of $[\text{kg s}^{-1} \text{ nucleon}^{-1} \text{ ster}^{-1}]$ for C^+ and H^+ , and in the final column we show the relative abundance of inner source H^+ to C^+ .

	λ (AU)	L (AU)	χ	$\frac{dm}{dt}(r_1; \text{C}^+)$	$\frac{dm}{dt}(r_1; \text{H}^+)$	$[\text{H}^+]/[\text{C}^+]$
1995 data: lat $< 25^\circ$	> 2	0.3	2.5	22	43,200	2000
1994 data: lat $> 45^\circ$	> 2	0.05	1.2	37	11,300	310

source ions. One conclusion from interstellar pickup ion studies is that the distributions are hemispheric, that is uniform in hemispheres centered on the magnetic field direction (1). The distributions appear to be highly anisotropic, however, with far more ions in the sunward than antisunward hemisphere. Since ions are picked in the sunward hemisphere, this suggests that the anisotropy in the pickup ions is caused by a difficulty for ions to scatter through 90° pitch-angle, where the pitch-angle is the angle between the instantaneous pickup ion velocity and the magnetic field direction.

The full transport equation for pickup ions under the assumption of hemispheric distributions has been written down and solved by (8, 10, 12). The starting point is that distributions are uniform in the sunward hemisphere, f_- , and in the antisunward hemisphere, f_+ . Here we simplify the transport equations by neglecting field aligned streaming and adiabatic focusing:

$$u \frac{\partial f_0}{\partial r} - \frac{2u}{3r} v \frac{\partial f_0}{\partial v} = \frac{\beta}{2} \left(\frac{r_1}{r} \right)^2 n_n(r) \frac{\delta(v-u)}{2\pi u^2} \quad (1)$$

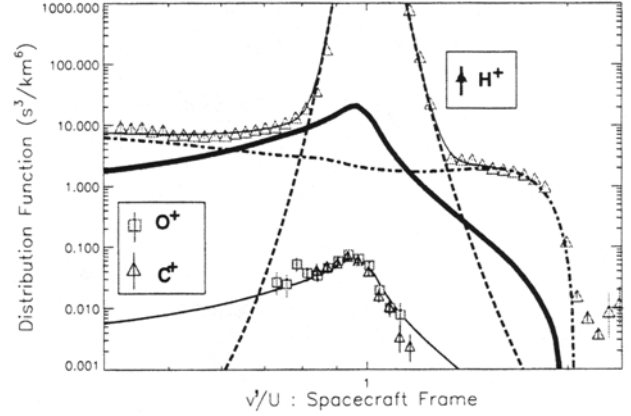
$$u \frac{\partial \Delta}{\partial r} - \frac{2u}{3r} v \frac{\partial \Delta}{\partial v} = -\frac{2\Delta}{\tau} - \frac{\beta}{2} \left(\frac{r_1}{r} \right)^2 n_n(r) \frac{\delta(v-u)}{2\pi u^2} \quad (2)$$

Here $f_0 = (f_+ + f_-)/2$ is the isotropic part of the distribution function and $\Delta = (f_+ - f_-)/2$ is the anisotropic part. The solar wind speed is denoted u , the ion speed in the solar wind frame is denoted v , and $\lambda = v\tau$ is the scattering mean free path. The radial distance is denoted r and r_1 denotes 1 AU. We have assumed that the solar wind executes a standard radial expansion. The production rate is given by $\beta(r_1/r)^2$ which implicitly neglects electron impact ionization. We assume the pickup ions are introduced in the wind with speed $v = u$. Given a constant mean free path, we obtain the following analytic solutions:

$$f_0 = \frac{3}{8\pi u^4} \beta r_1 \left(\frac{r_1}{r w^{3/2}} \right) n_n \left(r w^{3/2} \right) \quad (3)$$

$$\Delta = -f_0 \exp \left[-\frac{6r}{\lambda} w(1 - \sqrt{w}) \right] \quad (4)$$

The neglect of field-aligned streaming and adiabatic focusing can be justified based on the small speeds of inner source which have been adiabatically cooled due to



Source: N. Schwadron, University of Michigan

FIGURE 1. The inner source C^+ , O^+ , and H^+ distribution functions observed during all of 1994.

the usual betatron effect. This is a somewhat subtle assumption, but has been rigorously checked by comparing this solution with the results of a numerical model (10) which solves the complete transport equations.

For the inner source density profile we take,

$$n_n(r) = n_0 \exp \left(-\frac{L}{r} \right) \left(\frac{r_1}{r} \right)^\chi \quad (5)$$

where L characterizes inner radial maximum in the source, given by L/χ , and χ characterizes the radial spread of the grain source.

In Figures 1 and 2, the solid curves show results of the modeled distributions. The observed distributions have been integrated over extremely long periods ~ 1 year. Therefore multiple model runs were performed for heliospheric positions at many points along the Ulysses trajectory. In the lower panel of Figure 1 we see a comparison between the inner source model results and the C^+ and O^+ distributions. In the upper panel, we show comparisons for the H^+ distribution function. Several different populations are apparent in the H^+ distribution: i) the black dashed curve shows the solar wind protons, modeled here with a kappa function; ii) the grey dashed curve extending to twice the solar wind speed represents

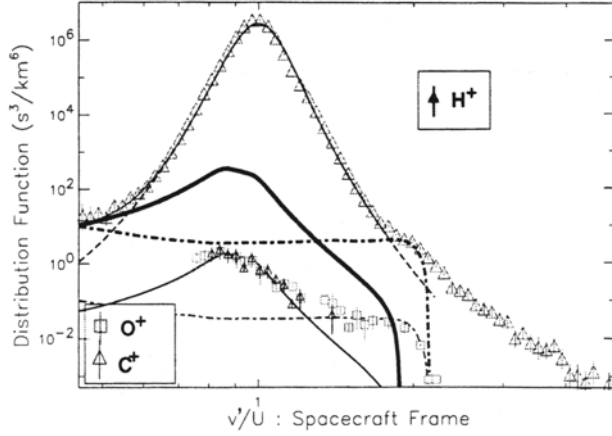


FIGURE 2. The inner source C^+ , O^+ , and H^+ distribution functions observed between day 30 and 90 of 1995.

the interstellar protons; and iii) the thick black curve represents the inner source ions. This figure shows definitively that inner source ions are observed in the proton spectra since the proton distribution in the speed range $0.6 < v'/u < 0.85$ could not be accounted for without a third distribution of ions.

In Figure 2, we show a similar comparison; however, it is apparent that interstellar O^+ is also observed in the lower distribution. The dashed curve in the lower distribution shows the interstellar O^+ contribution.

Interstellar O^+ could not be observed by Ulysses/SWICS in the fast solar wind, $u \sim 750$ km/s, since the upper energy threshold of SWICS, 60 keV, leads to an upper speed cutoff at $v/u = 1.1$. This cutoff explains why interstellar O^+ was not seen in Figure 1.

The parameters λ , L and χ used in these comparisons are shown in Table 1. Also listed in the Table is the net mass production rate per nucleon within a steradian solid angle element from the solar surface, r_0 , to $r_1 = 1$ AU,

$$\frac{dm}{dt}(r_1) = m_p \int_{r_0}^{r_1} dr r^2 \beta \left(\frac{r_1}{r}\right)^2 n_n(r) \quad (6)$$

where m_p is the proton mass. In the final column is the relative abundance of H^+ to C^+ , $[H^+]/[C^+]$.

CONCLUSIONS

The scattering mean free path obtained for the inner source ions suggests that they are essentially unscattered through 90° pitch-angle. This is consistent with long scattering mean free paths observed for interstellar pickup ions (6, 1, 10, 12). It is perhaps surprising that the scattering mean free path is still so large close to the Sun.

We note however that very large mean free paths have been obtained for scatter free electron events (see, (9)) which involve electrons with a similar rigidity to the inner source ions. Moreover, the inner source ions adiabatically cool as they propagate due to the usual betatron effect. Hence the long mean free path for inner source ions clearly indicates that scattering through 90° remains highly suppressed as the ions decrease their speed and therefore rigidity.

The radial distribution suggests that at high latitudes the inner source is very much like the dust grains, falling as $1/r$ and having an inner edge near 10 solar radii. At low latitudes, this similarity with the dust distribution breaks down. The low latitude source is both steeper and somewhat pushed out with respect to the high latitude source.

The latitudinal distribution suggested by this analysis is also interesting. The inner source H^+ appears to be more heavily concentrated near the ecliptic, while for C^+ and O^+ , the ions appear to be more heavily concentrated at high latitudes. Another factor is that the relative abundance $[H^+]/[C^+]$ suggests a universal abundance at low latitudes and a somewhat lower value at high latitudes. These facts taken together suggest an additional source of inner source C^+ and O^+ at high latitudes, perhaps due to interstellar grains.

The mere presence of inner source H^+ ions is significant since hydrogen is so much more abundant than the other species. One immediate consequence is the potential energetic importance of this inner source population in the solar wind. By working a simple calculation which follows, it is easy demonstrate that the inner source protons may carry a dominant pressure in the solar wind close to their source.

Consider the density of inner source O^+ derived from our fit to the O^+ distribution at high latitudes near $r_{\text{obs}} = 3$ AU, $n_O(r_{\text{obs}}) \sim 5.5 \cdot 10^{-7} \text{ cm}^{-3}$. If we project this density back to the source near $r_{\text{src}} = 0.3$ AU, we find

$$n_O(r_{\text{src}}) \sim \left(\frac{r_{\text{obs}}}{r_{\text{src}}}\right)^2 \frac{u - v_O(r_{\text{obs}})}{u - v_O(r_{\text{src}})} n_O(r_{\text{obs}}). \quad (7)$$

Here $v_O(r_{\text{obs}})$ is the average speed at which O^+ ions stream against the solar wind in the radial direction at $r = r_{\text{obs}}$, and $v_O(r_{\text{src}})$ is the inward streaming speed at $r = r_{\text{src}}$. We find from our fit distribution that $v_O(r_{\text{obs}}) \sim 80$ km/s. In the case that the O^+ distribution is highly anisotropic near the source, the quantity, $u - v_O(r_{\text{src}})$ may be quite small. In this illustrative example, we take, $u - v_O(r_{\text{src}}) \sim 10$ km/s yielding, $n_O(r_{\text{src}}) \sim 4 \cdot 10^{-3} \text{ cm}^{-3}$. Factoring in the relative abundance of H^+ to O^+ of ~ 310 , we find a density of inner source H^+ , $n_H \sim 1.2 \text{ cm}^{-3}$ and a pressure,

$$P_H(r_{\text{src}}) \sim m_p n_H(r_{\text{src}}) u^2 \sim 1.2 \cdot 10^{-8} \text{ erg/cm}^3. \quad (8)$$

As a comparison, we find with a 4 nT magnetic field at 1 AU, a magnetic pressure given by

$$\frac{B^2}{8\pi}(r_{\text{src}}) \sim 4.3 \cdot 10^{-9} \text{erg/cm}^3, \quad (9)$$

and a typical solar wind thermal pressure given by,

$$P_{\text{sw}} \sim 6 \cdot 10^{-9} \text{erg/cm}^3. \quad (10)$$

In other words, if the inner source ions are highly anisotropic close to the Sun, the pressure P_H may exceed both the magnetic field pressure and the solar wind thermal pressure.

REFERENCES

1. Fisk, L. A., Schwadron, N. A., and Gloeckler, G., *Geophys. Res. Lett.* **24**, (1997) 93.
2. Geiss, J., Gloeckler, G., Fisk, L. A., and von Steiger, R., *J. Geophys. Res.* **100**, (1995) 23373–23377.
3. Gloeckler, G., Fisk, L. A., Geiss, J., Schwadron, N. A., and Zurbuchen, T. H., *Geophys. Res. Lett.* In Press.
4. Gloeckler, G., and Geiss, J., *Space Science Reviews* **85**, (1999) 127.
5. Gloeckler, G., Geiss, J., Balsiger, H., Bedini, P., Cain, J. C., Fischer, J., Fisk, L. A., Galvin, A. B., Gliem, F., Hamilton, D. C., Hollweg, J. V., Ipavich, F. M., Joos, R., Livi, S., Lundgren, R., Mall, U., McKenzie, J. F., Ogilvie, K. W., Ottens, F., Rieck, W., Tums, E. O., von Steiger, R., Weiss, W., and Wilken, B., *Astron. Astrophys. Suppl. Ser.* **92**, (1992) 267–289.
6. Gloeckler, G., Schwadron, N. A., Fisk, L. A., and Geiss, J., *Geophys. Res. Lett.* **22**, (1995) 2665.
7. Gruntman, M., *J. Geophys. Res.* **101**, (1996) 15555.
8. Isenberg, P. A., *J. Geophys. Res.* **102**, (1997) 4719.
9. Palmer, I. D., *Rev. Geophys.* **20**, (1982) 335.
10. Schwadron, N. A., *J. Geophys. Res.* **103**, (1998) 20643.
11. Schwadron, N. A., Gloeckler, G., Fisk, L. A., Geiss, J., and Zurbuchen, T. H., *Geophys. Res. Lett.* In Press.
12. Schwadron, N. A., Zurbuchen, T. H., Fisk, L. A., and Gloeckler, G., *J. Geophys. Res.* In Press.